

# Thermal and magnetic instability near the percolation threshold of $\text{Nd}_{0.5}(\text{Ca},\text{Sr})_{0.5}\text{MnO}_3$

C. W. Chang,\* A. K. Debnath,† and J. G. Lin‡

Center for Condensed Matter Science, National Taiwan University, Taipei, Taiwan

(Received 13 July 2001; published 17 December 2001)

We report the observation of an instability phenomena in  $\text{Nd}_{0.5}(\text{Ca},\text{Sr})_{0.5}\text{MnO}_3$  for cyclic runs between 300 and 10 K through resistivity, thermopower, and magnetization measurements. The instability is especially dramatic when the concentration of Sr is near the metal/insulator percolation threshold, and it manifests itself in the delicate balance between the external magnetic field and the intrinsic instability. We also demonstrate an effective way of turning the metallic or insulating phases by switching off the external field at particular temperatures. Further studies on time-relaxation effect reveal that the change of resistivity is logarithmic-time dependent and it occurs only within a small temperature range, suggesting that the transition is not only thermal assisted but also magnetically correlated.

DOI: 10.1103/PhysRevB.65.024422

PACS number(s): 75.30.Kz, 71.27.+a, 71.30.+h, 71.45.Lr

## INTRODUCTION

The interplay of the double-exchange interaction and the charge/orbital ordering results in a complicated phase diagram for colossal magnetoresistive (CMR) oxides  $R_{1-x}A_x\text{MnO}_3$  ( $R$ =rare-earth elements,  $A$ =Ca, Sr, Ba).<sup>1</sup> Generally, the double-exchange interaction favors a ferromagnetic metallic state whereas the charge/orbital ordering is accompanied with an antiferromagnetic insulating state via the superexchange interaction. The competition among interactions is especially robust for  $x=0.5$ , in which the coexistence of ferromagnetic and antiferromagnetic domains has been observed.<sup>2</sup> The competition also leads to some intriguing phenomena such as thermal hysteresis of resistivity, thermopower, lattice structure, etc.<sup>3,4</sup> By varying the radius of A-site ion,  $\langle r_A \rangle$ , a large shift of the charge-ordering temperature ( $T_{\text{co}}$ ) has been observed. Studies on the  $\langle r_A \rangle$  dependency of the metal-insulator transition temperature ( $T_m$ ) and  $T_{\text{co}}$  for  $\text{La}_{0.5}(\text{Ca},\text{Sr})_{0.5}\text{MnO}_3$ , and  $\text{Pr}_{0.5}(\text{Ca},\text{Sr})_{0.5}\text{MnO}_3$  systems can be summarized in Fig. 1.<sup>5,6</sup> Generally, for  $\langle r_A \rangle > 0.12$  nm,  $T_m$  increases and  $T_{\text{co}}$  decreases with increasing

$\langle r_A \rangle$ . For  $\langle r_A \rangle < 0.12$  nm a larger lattice distortion and the Mn-O-Mn bond angle bending leads to a suppression of the ferromagnetic interaction and consequently, the charge-ordering state dominates.<sup>7</sup> The simultaneous change of  $T_m$  and  $T_{\text{co}}$  has been viewed as a direct consequence of the competition between ferromagnetism and charge-ordering interaction.<sup>3</sup>

However, the empirical relation is not applicable for  $R=\text{Nd}$  systems. Actually, as displayed in Fig. 1, the  $T_m$ 's of Nd-based systems "intrude" into the region where the charge-ordering state should dominate. For example, in  $(\text{Nd},\text{Sm})_{1/2}\text{Sr}_{1/2}\text{MnO}_3$  systems, the metallic states appear at a rather low-temperature range.<sup>6</sup> Moreover, for  $\text{Nd}_{0.5}\text{Ca}_{0.5-y}\text{Sr}_y\text{MnO}_3$  with  $y < 0.2$ , it does not show a charge-ordering transition for  $\langle r_A \rangle < 0.12$  nm; instead, remains in the ferromagnetic metallic state even at low temperature. Such an anomalous recovery of the ferromagnetic-metallic state and a suppression of the charge-ordering insulating state at small  $\langle r_A \rangle$  remain a mystery. From another aspect, the pressure effect on  $\text{Nd}_{0.125}(\text{Sn}_{0.875})_{1/2}\text{Sr}_{1/2}\text{MnO}_3$  or  $\text{Nd}_{0.5}\text{Sr}_{0.5}\text{MnO}_3$  is opposite to that of typical charge-ordering compound  $\text{Pr}_{0.5}\text{Ca}_{0.5}\text{MnO}_3$ .<sup>8-10</sup> In addition, an atypical huge positive magnetovolume effect has been observed in  $\text{Nd}_{0.5}\text{Sr}_{0.5}\text{MnO}_3$ .<sup>11</sup> Furthermore, unlike  $\text{Pr}_{0.5}\text{Sr}_{0.5}\text{MnO}_3$ , three different magnetic phases have been observed to coexist in  $\text{Nd}_{0.5}\text{Sr}_{0.5}\text{MnO}_3$  below 125 K.<sup>12</sup> Naturally, these anomalies raise interests to investigate the underlying mechanism that leads to the notable deviation of  $T_m$  and  $T_{\text{co}}$  in the Nd-based systems as seen in Fig. 1. Although some mechanisms such as the striction-coupled interaction have been proposed to account for these deviations,<sup>13</sup> a complete and satisfied model is still required for all  $x=0.5$  system.

In order to unravel the mysterious characteristics of the Nd-based system, we have made  $\text{Nd}_{0.5}(\text{Ca},\text{Sr})_{0.5}\text{MnO}_3$  samples with Sr concentrations from zero to 0.5. Interestingly, we discovered that the resistivity changes significantly with cyclic runs between room temperature and low temperature. This effect is especially large when the Sr concentration is close to the metal-insulator transition threshold. Data of thermopower and magnetization also show a similar instability behavior. Magnetoresistance measurements fur-

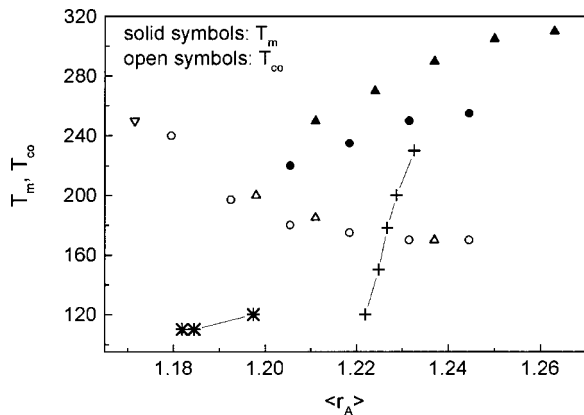


FIG. 1.  $T_m$  (solid symbols) and  $T_{\text{co}}$  (open symbols) as a function of  $\langle r_A \rangle$ . Data for  $\text{La}_{0.5}(\text{Ca},\text{Sr})_{0.5}\text{MnO}_3$  (triangles) and  $\text{Pr}_{0.5}(\text{Ca},\text{Sr})_{0.5}\text{MnO}_3$  (circles) are taken from Refs. 3 and 4.  $T_m$  for  $(\text{Nd},\text{Sm})_{1/2}\text{Sr}_{1/2}\text{MnO}_3$  (crosses, from Ref. 5) and  $\text{Nd}_{0.5}(\text{Ca},\text{Sr})_{0.5}\text{MnO}_3$  (stars, from present study) are also shown for comparison.

ther demonstrate that the instability is intrinsic, and the temperature-dependent time-relaxation effect suggests that the instability is thermal assisted and is magnetically correlated.

### EXPERIMENTS

Polycrystalline samples of  $\text{Nd}_{0.5}\text{Ca}_{0.5-y}\text{Sr}_y\text{MnO}_3$  were synthesized by the solid-state reaction of high-purity powders of  $\text{Nd}_2\text{O}_3$ ,  $\text{SrCO}_3$ ,  $\text{CaCO}_3$ , and  $\text{MnCO}_3$ . The  $\text{Nd}_2\text{O}_3$  powders were first dried at  $900^\circ\text{C}$  for 1 h, then were mixed with other powders in an appropriate molar ratio and heated at ambient pressure to  $1200^\circ\text{C}$  for 16 h with an increasing rate of  $5^\circ\text{C}/\text{min}$ . Then the sample was cooled to  $150^\circ\text{C}$  in furnace with decreasing rate  $\sim -5^\circ\text{C}/\text{min}$ . Again the mixed powders were well ground, pelletized, and heated at  $1400^\circ\text{C}$  for 16 h with the same heating rate. X-ray diffraction data (XRD) had confirmed that all compounds were single phases. Samples from different pellets were used for different measurements. Standard four-probe method with indium-soldered contacts was used to obtain resistivity. The absolute thermopower ( $S$ ) of the sample was obtained by a dc method and was calibrated against a Pb standard. A Cu/Constantan thermocouple was used to detect the temperature gradient that was kept in a range of  $0.8\sim 1.2$  K. Each thermal cycle for resistivity and thermal power takes 2 and 14 h, respectively. Magnetization was measured by a superconducting quantum interference device (SQUID) (quantum design) magnetometer in the temperature range  $6\sim 300$  K under 100 Oe fields. For comparison, we kept the sample at room temperature for more than 1 month and repeat the measurements. Our results clearly demonstrate that the observed thermal-instability effects are not due to chemical decomposition effect.

### RESULTS AND DISCUSSION

Figure 2 shows the resistivity ( $\rho$ ) vs temperature ( $T$ ) for  $y=0.09$  and  $0.1$  for successive eight cyclic runs between  $295$  and  $10$  K. Both cooling and warming curves displays thermal instability, but only warming curves are shown for clarity. It is evident that for both  $y=0.09$  and  $0.1$ ,  $\rho$  keeps on increasing for increasing cyclic runs. For  $y=0.09$ ,  $T_m$  shifts from  $145$  to  $108$  K after eight runs. For  $y=0.1$ , the shift of  $T_m$  is less, about  $10$  K.

More drastic change is observed for  $y=0.08$ , as plotted in Fig. 3. The resistivity shows an insulator-metal transition at  $65$  K for the 1st run, and it remains an almost temperature-independent value below  $25$  K. It is worthy to note that though  $\rho(T)$  shows metallic behavior at low temperature, residual resistivity is rather high. Comparing Fig. 2 with Fig. 3, it is surprising that  $\rho$  value at  $11$  K changes a lot with a slight change of Sr-content. The anomalous high-resistivity metallic state and the doping-sensitive behavior of resistivity are the evidences of the percolative nature exhibited universally in the charge-ordered CMR oxides.<sup>14,15</sup> Further indications come from the transitional behaviors with different cyclic runs as shown in Fig. 3.  $\rho(T)$  displays a jump at the 2nd to 4th runs, and the residual resistivity gets larger, and fi-

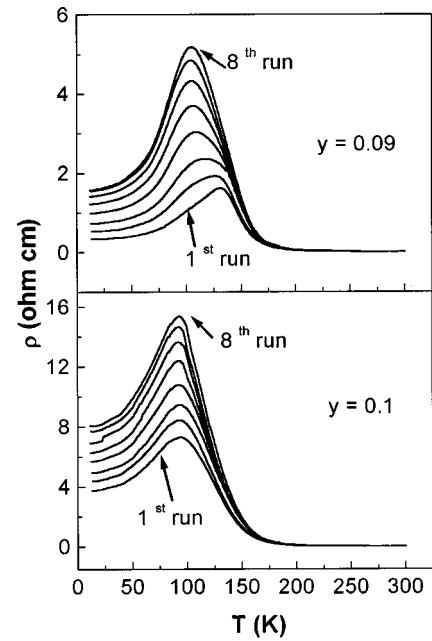


FIG. 2. Resistivity vs temperature for  $y=0.09$  and  $0.1$  at different cyclic runs. Only warming curves are shown for clarity.

nally, the sample becomes an insulator at the 5th and 6th runs.

Although the sample of  $y=0.08$  becomes insulating after several cyclic runs, applying a magnetic field can recover the insulator-metal transition as well as the low-resistivity state. As shown in Fig. 4, the insulator-metal transition is recovered under  $0.5$  and  $1.3$  T. Considering it requires a high field of  $5$  T to collapse the charge-ordering state in  $\text{Pr}_{0.5}(\text{Sr,Ca})_{0.5}\text{MnO}_3$  and  $\text{Nd}_{0.5}\text{Ca}_{0.5}\text{MnO}_3$ ,<sup>3,24</sup> the low-field-induced recovery of the metallic state for  $\text{Nd}_{0.5}(\text{Sr,Ca})_{0.5}\text{MnO}_3$  suggests that the instability is spin dependent. Figure 4 also demonstrates that the observed instability is not due to chemical decomposition effect otherwise the insulator-metal transition should not be recovered by magnetic field.

Correspondingly, the intrinsic instability manifests itself in the thermopower behavior with different cyclic runs. Since the cooling/warming rates for resistivity and ther-

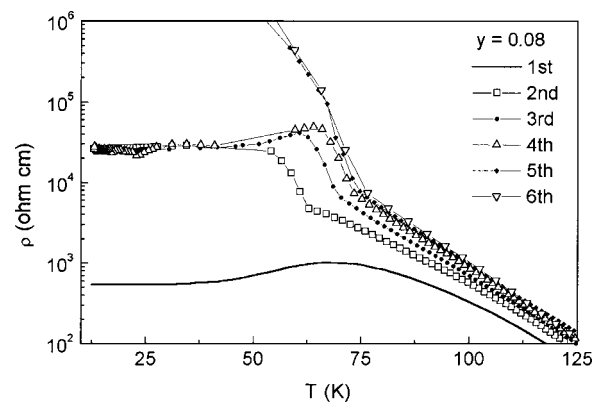


FIG. 3. Resistivity vs temperature for  $y=0.08$  at different cyclic runs. Only cooling curves are shown for clarity.

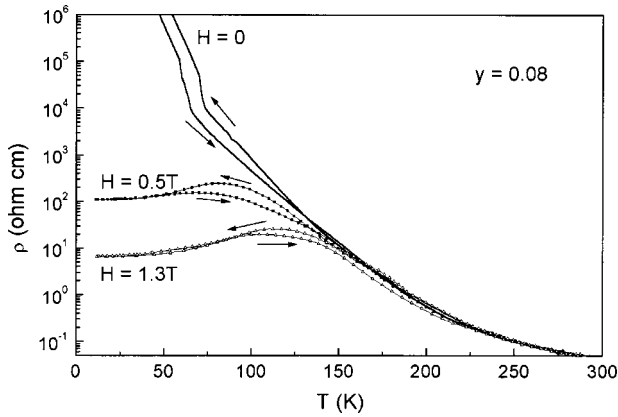


FIG. 4. Field dependent  $\rho T$  for  $y=0.08$ . The metal-insulator transition is recovered after applying magnetic field.

mopower measurements are not exactly the same, we do not intend to compare the corresponding cyclic runs for different measurements. The thermopower shows concave curves both for cooling and warming processes. In Fig. 5, only the cooling processes are shown. With decreasing temperature, the absolute thermopower ( $S$ ) of  $y=0.08$  shows a transition to a smaller value (less negative) similar to the behavior of  $y=0.5$  (see the dash line). After cyclic runs,  $S(T)$  of  $y=0.08$  is more negative and its high-temperature slope becomes larger (see three solid symbols). For the 3rd run,  $S(T)$  shows a transition at 130 K, but the high-temperature part of curve is similar to that of  $y=0.0$  (see the solid line). Since it has been demonstrated that for percolative transport behavior, the effective thermopower can be formulated by a combination of metallic and insulating components,<sup>15</sup> the similarity in the thermopower of the 3rd run and that of  $y=0.0$  clearly indicates that the instability is intrinsically a percolative transition originating from the growth/depletion of insulating/metallic domains.

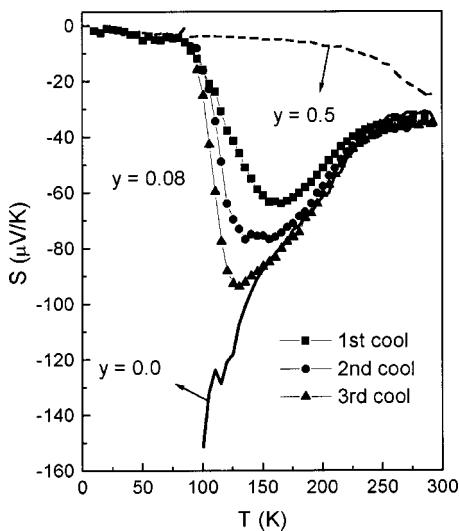


FIG. 5. Thermopower vs temperature at three successive cyclic runs for  $y=0.08$ . Only cooling curves are shown for clarity. Thermopower data of  $y=0.0$  (dashed line) and  $0.5$  (solid line) are also shown for comparison.

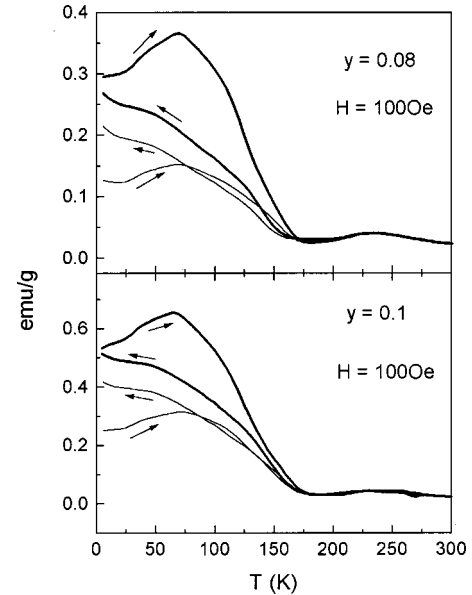


FIG. 6. Magnetization as a function of temperature for  $y=0.08$  (upper panel) and  $0.1$  (lower panel). Each panel contains two sets of data bold lines for the fresh sample and thin lines for the liquid  $N_2$  treated one.

To investigate the magnetic response for the cyclic runs, the samples for magnetization measurements were separated into two groups, one of them (fresh sample) was directly put into SQUID for the magnetization measurement, and the other one ( $IN_2$  treated) was dipped into liquid  $N_2$  then warmed up to the room temperature for seven times to simulate the cyclic runs conditions as mentioned above. For the magnetization measurement, the samples were first zero field cooled, then warming up to 295 K under 100 Oe, and again cooled down to 5 K under 100 Oe. The magnetic field of 100 Oe is chosen not to affect the intrinsic change resulting from cyclic runs. Figure 6 shows the magnetization behavior for  $y=0.08$  and  $0.1$ . The enhanced magnetization suggests that a ferromagnetic state emerges below 170 K. It is worth noting that for both  $y=0.08$  and  $0.1$ , the low-temperature magnetization for the fresh samples (bold lines) exhibit larger moments than those of the  $IN_2$  treated samples (thin lines). The observed large reduction of magnetic moments consists with the previous data that increasing cyclic runs increases the population of the insulating domains, i.e., the charge-ordering (antiferromagnetic) components.

Based on our data, the instability is attributed to the competition between metallic (ferromagnetic) and insulating (antiferromagnetic) domains. In fact, we have found that the delicate balance between the instability and the external magnetic field can be carefully manipulated by the following method. First, the sample was field cooled under 1.3 T and then the field was switched off at the particular temperature ( $T_{\text{off}}$ ). Figure 7 shows the resistivity behavior with respect to different  $T_{\text{off}}$ . For  $T_{\text{off}}=11$  K, the resistivity clearly displays a field-induced recovery of the insulator-metal transition as discussed earlier. For  $T_{\text{off}}<130$  K, the resistivity curves show metallic behaviors at low temperature, and  $T_m$  decreases with increasing  $T_{\text{off}}$ . For  $T_{\text{off}}=150$  K, there is a

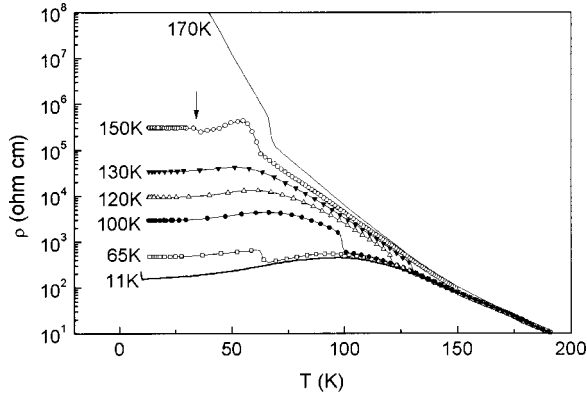


FIG. 7.  $\rho$  as a function of switching temperature  $T_{\text{off}}$ . The arrow displayed in the curve of  $T_{\text{off}}=150$  denotes a transition to a high-resistance state at 33 K.

sharp insulator to metal transition at 55 K. In addition, the unstable nature of the metallic state for  $T_{\text{off}}=150$  K makes itself switch to a higher resistance state (as denoted by the arrow in Fig. 7) and the resistivity becomes nearly temperature independent below 33 K. The interesting behaviors for  $T_{\text{off}}=150$  K demonstrate a delicate balance between the external field and the intrinsic instability. For  $T_{\text{off}}=170$  K, a jump of resistivity is evident at 70 K. The jump of resistivity has been considered to be a dispensable feature of the charge-ordering state,<sup>16</sup> hence it is mostly possible that the insulating state originate from charge ordering.

Up to now we have demonstrated that the observed instability is not a chemical decomposition effect; besides, the sample is rather stable at room temperature. It is then natural to ask whether the instability is effective at some particular temperature range. More importantly, a temperature-dependent relaxation should grant us more information regarding its correlation with the thermal activation energy.

For the time-relaxation measurement, each fresh sample was cooled down to specific temperatures and maintained for several hours to record the resistivity change with respect to time. The percentage resistivity change is defined as

$$\frac{\Delta\rho}{\rho} = 100 \times \frac{\rho(t) - \rho(0)}{\rho(0)}, \quad (1)$$

where  $t$  is the time measured after the sample was cooled to a specific temperature. Figure 8 shows  $\Delta\rho/\rho$  vs time at different temperature. We find that the data in Fig. 8 can be fitted by the following equation:

$$\frac{\Delta\rho(t)}{\rho} = A \ln t + \text{const}, \quad (2)$$

where  $A$  is a constant for a fixed temperature. The linear dependence of a logarithm of time is often observed in soft ferromagnets and spin glass.<sup>17,18</sup> In fact, the relation of Eq. (2) has also been observed in CMR oxides.<sup>19,20</sup> From Fig. 8, it is clear that the resistivity change is highly dependent on the temperature. For  $T=11$  K, there is negligible  $\Delta\rho/\rho$ . For  $T=50$  K, the slope is negative rather than positive. Since the thermal hysteresis for  $y=0.08$  (shown in Fig. 4) shows that

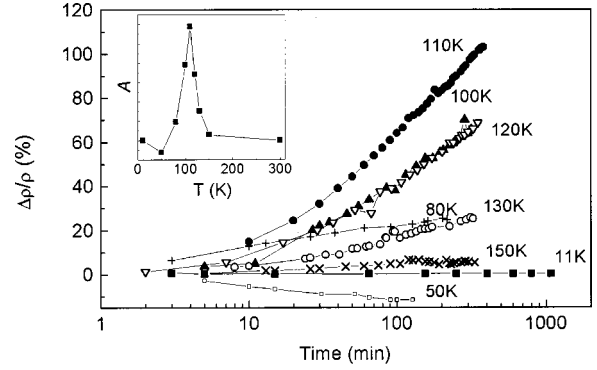


FIG. 8. Resistivity change as a function of time at different temperatures for  $y=0.08$ . Inset shows the slopes of  $\Delta\rho/\rho$  vs  $\ln t$  at different temperatures.

the warming curve has lower resistivity than that of the cooling curve, it is possible that the origin of the negative slope results from the thermal hysteresis rather than the instability effect.<sup>21</sup> More interestingly, for  $T=100$  K, 110 K, and 120 K, their slopes are larger than those at other temperatures, demonstrating that not only the time-relaxation effect is temperature dependent, but also effective within a small temperature range only. Inset of Fig. 8 shows the slope ( $A$ ) vs temperature. For a simple thermal-activated behavior,  $A$  should be a monotonic increasing function of temperature. However,  $A$  is suppressed at high temperature suggests that another mechanism must be introduced to account for the temperature dependence of  $A$ .<sup>22</sup> According to the double-exchange mechanism, there is a universal correlation between ferromagnetic transition and insulator-metal transition in CMR oxides. Therefore, it is essential to include the magnetization ( $M$ ) as an independent parameter, i.e.,  $A = A(M, T)$ .<sup>22</sup> However, our preliminary study indicates that  $A$  is not a simple function of  $M$  and  $T$ . Further studies are required to understand the temperature/magnetization-dependent instability. It is worthy to note that the change of the resistivity shown in Fig. 8 is much smaller than the effect for cyclic runs (Fig. 3) within the same time scale. The contrast between the changes of the resistivity shown in Fig. 3 and Fig. 8 suggests that the effect for cyclic runs is equivalent to a thermal annealing effect for material processing, i.e., after the thermal treatment (cyclic runs), the sample is transformed into an energetically favorable state (insulating state). The result of this thermal annealing effect is consistent with our recent discovery of the current-assisted annealing effect for  $y=0.1$ .<sup>23</sup>

It is natural to ask what is the underlying driving force for the observed instability. Based on our data, it is sure that the insulating state is energetically more favorable. Considering that the sample of  $y=0.08$  is similar to  $\text{Nd}_{0.5}\text{Ca}_{0.5}\text{MnO}_3$  in composition, we may assign the energetically favorable insulating state of  $y=0.08$  to be the CE-type orbital ordering state, as the low-temperature state of  $\text{Nd}_{0.5}\text{Ca}_{0.5}\text{MnO}_3$ .<sup>24</sup> Actually, as shown in Fig. 8,  $\Delta\rho/\rho$  is barely observable below 150 K which is exactly the onset of CE-type ordering ( $T_N \sim 150$  K) for  $\text{Nd}_{0.5}\text{Ca}_{0.5}\text{MnO}_3$ .<sup>24</sup> It is then reasonable to attribute the observed instability to the competition between

the ferromagnetic and the CE-type orbital ordering. The magnetization instability demonstrates a reduction of the ferromagnetic domains, which also suggests that the instability is due to a gradual depletion of ferromagnetic domains and a growth of CE-type antiferromagnetic domains. Although three kinds of orbital ordering has been observed in  $\text{Nd}_{0.5}\text{Sr}_{0.5}\text{MnO}_3$ , direct evidences from the neutron diffraction suggest that the CE-type ordering is more fragile to external field than that of  $A$ -type orbital ordering.<sup>12</sup> Thus, the field-induced recovery in  $y=0.08$  should be resultant effect from the collapsing of the CE-type ordering under low field. However, it remains to be answered why the ferromagnetism emerges at these Nd-based compounds with such a small  $\langle r_A \rangle$  as shown in Fig. 1. Though previous works reveal that Nd-system exhibits unusual striction-coupled effect, a successful model has not yet been established, which should interpret not only the typical behaviors of  $\text{La}_{0.5}(\text{Ca},\text{Sr})_{0.5}\text{MnO}_3$  and  $\text{Pr}_{0.5}(\text{Ca},\text{Sr})_{0.5}\text{MnO}_3$ , but also the unusual magnetovolume or high-pressure effect in Nd-based systems. Even for Nd-based samples with  $x \neq 0.5$ , they still show atypical behaviors.<sup>25</sup> Besides, for other rare-earth dopants such as  $(\text{La},\text{Sm})_{0.5}\text{Sr}_{0.5}\text{MnO}_3$  and  $(\text{Pr},\text{Gd})_{0.5}\text{Sr}_{0.5}\text{MnO}_3$  systems, similar deviations in the phase diagram have been observed.<sup>26</sup> Therefore, it is possible that origin of the anomaly for these systems is a special electronic configuration of rare-earth ions.

In summary, we have observed a gradual transition from a metallic/ferromagnetic to an insulating/antiferromagnetic state from the cyclic measurements of resistivity, magnetization, and thermopower in  $\text{Nd}_{0.5}\text{Ca}_{0.5-y}\text{Sr}_y\text{MnO}_3$ . The insta-

bility is especially dramatic for  $y=0.08$ , which is close to the metal-insulator percolation concentration. With applying magnetic field, we find that the instability is suppressed and the insulator-metal transition is recovered. Therefore, the observed instability is not due to a decomposition effect. We also find that the delicate balance of the external field and the intrinsic instability can be manipulated by switching the field at a particular temperature. In some cases, the resistivity shows a sharp drop at  $T_m$ , while in other cases, a resistivity jump features as a charge-ordering transition. Furthermore, time-relaxation effect shows a logarithmic-temperature dependency. Below 110 K, the relaxation is enhanced with increasing temperature, suggesting a thermal-assisted origin. However, it is suppressed above 120 K, indicating that the instability is magnetically correlated. The observed instability for cyclic runs is possibly explained by a gradual transition from a ferromagnetic state to the CE-type ordering in origin, and an annealing effect in character. In all aspects, the Nd-based system behaves differently from other typical compounds such as  $\text{Re}=\text{La}$  and  $\text{Pr}$  systems. We thus suggest that these unusual behaviors may be correlated with the electronic configuration of the  $\text{Nd}^{3+}$  ion.

#### ACKNOWLEDGMENT

We would like to thank Director T. J. Chuang for his consistent support and Dr. R. Gundakaram for the XRD measurements. This work is supported by the National Science Council and the Department of Education of Republic of China under Grants Nos. 89-N-FA01-2-4-5 and NSC 89-2112-M-002-081.

\*Present address: Department of Physics, University of California at Berkeley, Berkeley, California 94720.

†Permanent address: Technical Physics and Prototype Engineering Division, Bhabha Atomic Research Center, Trombay, Mumbai-400 085, India.

‡Corresponding author: Center for Condensed Matter Science, National Taiwan University No. 1, Sec. 4, Rd. Roosevelt, Taipei 106, Taiwan. FAX: 886-2-23655404. Email address: jglin@ccms.ntu.edu.tw

<sup>1</sup>For a review, see *Colossal Magnetoresistance, Charge Ordering, and Related Properties of Manganese Oxides*, edited by C. N. R. Rao and Raveau (World Scientific, Singapore, 1998).

<sup>2</sup>For a review regarding the charge-ordering phenomena, see C. N. R. Rao, A. Arulraj, A. K. Cheetham, and B. Raveau, *J. Phys.: Condens. Matter* **12**, R83 (2000).

<sup>3</sup>C. W. Chang, C. Y. Huang, M. F. Dai, and J. G. Lin, *J. Phys.: Condens. Matter* **12**, 9425 (2000).

<sup>4</sup>S. Krupička, M. Maryško, Z. Jiráček, and J. Hejtmánek, *J. Magn. Magn. Mater.* **206**, 45 (1999).

<sup>5</sup>A. Sundaresan, P. L. Paulose, R. Mallik, and E. V. Sampathkumar, *Phys. Rev. B* **57**, 2690 (1998).

<sup>6</sup>H. Kuwahara, Y. Moritomo, Y. Tomioka, A. Asamitsu, M. Kasai, and Y. Tokura, *J. Appl. Phys.* **81**, 4954 (1997).

<sup>7</sup>P. V. Vanitha, P. N. Santhosh, R. S. Shingh, C. N. R. Rao, and J. P. Attfield, *Phys. Rev. B* **59**, 13 539 (1999).

<sup>8</sup>Y. Tokura, H. Kuwahara, Y. Moritomo, Y. Tomioka, and A. Asamitsu, *Phys. Rev. Lett.* **76**, 3184 (1996).

<sup>9</sup>A. S. Roy, A. Husmann, T. F. Rosenbaum, and J. F. Mitchell, *Phys. Rev. B* **63**, 094416 (2001).

<sup>10</sup>Y. Moritomo, H. Kuwahara, Y. Tomioka, and Y. Tokura, *Phys. Rev. B* **55**, 7549 (1997).

<sup>11</sup>R. Mahendiran, M. R. Ibarra, A. Maignan, F. Millange, A. Arulraj, R. Mahesh, R. Raveau, and C. N. R. Rao, *Phys. Rev. Lett.* **82**, 2191 (1999).

<sup>12</sup>C. Ritter, R. Mahendiran, M. R. Ibarra, L. Morellon, A. Maignan, B. Raveau, and C. N. R. Rao, *Phys. Rev. B* **61**, R9229 (2000).

<sup>13</sup>H. Kuwahara, Y. Tomioka, Y. Moritomo, A. Asamitsu, M. Kasai, R. Kumai, and Y. Tokura, *Science* **272**, 80 (1996).

<sup>14</sup>M. Uehara, S. Mori, C. H. Chen, and S.-W. Cheong, *Nature (London)* **389**, 560 (1999).

<sup>15</sup>K. H. Kim, M. Uehara, C. Hess, P. A. Sharma, and S.-W. Cheong, *Phys. Rev. Lett.* **84**, 2961 (2000).

<sup>16</sup>H. Kuwahara, Y. Tomioka, A. Asamitsu, Y. Moritomo, and Y. Tokura, *Science* **270**, 961 (1995).

<sup>17</sup>R. Street and J. C. Wolley, *Proc. Phys. Soc., London, Sect. A* **62**, 562 (1949).

<sup>18</sup>J. A. Mydosh, *Spin Glass: An Experimental Introduction* (Taylor and Francis, London, 1993).

<sup>19</sup>A. Anane, J.-P. Renard, L. Reversat, C. Dupas, P. Veillet, M. Viret, L. Pinsard, and A. Revcolevschi, *Phys. Rev. B* **59**, 77 (1999).

<sup>20</sup>M. Roy, J. F. Mitchell, and P. Schiffer, *J. Appl. Phys.* **87**, 5831 (2000).

- <sup>21</sup>N. A. Babushkina, L. M. Belova, D. I. Khomskii, K. I. Kugel, O. Yu. Gorbenco, and A. R. Kaul, *Phys. Rev. B* **59**, 6994 (1999).
- <sup>22</sup>L. M. Fisher, A. V. Kalinov, S. E. Savel'ev, I. F. Voloshin, and A. M. Balbashov, *J. Phys.: Condens. Matter* **10**, 9769 (1998).
- <sup>23</sup>C. W. Chang, A. K. Debnath, and J. G. Lin, *J. Appl. Phys.* (to be published).
- <sup>24</sup>M. Tokunaga, N. Miura, Y. Tomioka, and Y. Tokura, *Phys. Rev. B* **57**, 5259 (1998).
- <sup>25</sup>J.-S. Zhou, W. Archibald, and J. B. Goodenough, *Nature (London)* **381**, 770 (1996).
- <sup>26</sup>F. Damay, C. Martin, A. Maignan, and B. Raveau, *J. Appl. Phys.* **82**, 6181 (1997).